HOSTED BY

ELSEVIER

Alexandria University

Alexandria Engineering Journal

www.elsevier.com/locate/aej
www.sciencedirect.com

CrossMark

ORIGINAL ARTICLE

Geometrical optimization of a swirling Savonius wind turbine using an open jet wind tunnel

Abdullah Al-Faruk *, **Ahmad Sharifian**

Computational Engineering and Science Research Centre (CESRC), University of Southern Queensland, Toowoomba, Queensland 4350, Australia

Abstract   It has been suggested that waste heats or naturally available heat sources can be utilized to produce swirling flow by a design similar to that of split channels which is currently used to initiate fire whirls in laboratories. The new design combines the conventional Savonius wind turbine and split channel mechanisms. Previous computational and preliminary experimental works indicate a performance improvement in the new design (named as swirling Savonius turbine) compared to the conventional Savonius design. In this study, wind tunnel experiments have been carried out to optimize the swirling Savonius turbine geometry in terms of maximum power coefficient by considering several design parameters. The results indicate that the blade overlap ratio, hot air inlet diameter and the condition of the top end plate have significant influence on power and torque coefficients, while a larger aspect ratio and closed top end plate have some favourable effects on the performance. The optimum configuration has been tested in four different wind velocities to determine its influence on the performance, and power coefficients were found to be higher in high wind velocities. The performance comparison of optimum configuration with conventional Savonius rotor showed an increase of 24.12% in the coefficient of power.

1. Introduction

Being an energy source of low impact on the environment, low effects on health, and negligible safety issues, the demand for wind power has been increasing exponentially in recent years [1]. Moreover, wind energy is abundantly available in the

Earth's atmosphere, can be locally converted, and can thus help in reducing our reliance on fossil fuels. Until now, Horizontal Axis Wind Turbines (HAWTs) have played a primary role in response to this demand. The HAWTs can provide large power outputs, but it needs greater wind velocities and often generates low-frequency noise that can be harmful. In contrast, Vertical Axis Wind Turbines (VAWTs) are free from these environmental problems, resulting in the recent expansion of their use in urban environments. Savonius turbine is known as the most quiet wind power source among the wind turbines because the blades run at a speed of the same order as the wind velocity e.g. tip speed ratio $\gamma \approx 1$ [2]. Therefore, it can be employed to generate on-site electricity in city

* Corresponding author at: Z Block, Level 4, USQ, West Street, Toowoomba 4350, Australia.
E-mail addresses: abdullah.alfaruk@usq.edu.au, alfaruk.bd@gmail.com (A. Al-Faruk).

Nomenclature

C_P	coefficient of power
C_T	coefficient of torque
d	hot air inlet diameter (m)
d_w	nylon wire diameter (m)
D	diameter of rotor (m)
D_{ep}	end plate diameter (m)
D_{sh}	shaft diameter of rotor (m)
e	blade overlap distance (m)
H	height of rotor (m)
ID	inside diameter of blade pipe (m)
OD	outside diameter of blade pipe (m)
P	mechanical power (W)
Re	$(= \frac{UD}{v})$ Reynolds number
S	spring balance reading (N)
T	rotor torque (Nm)
U	wind velocity (m/s)
W	dead weight of dynamometer (N)

Greek letters

β	$(= \frac{e}{ID})$ blade overlap ratio
γ	tip speed ratio
ε	relative uncertainty
θ	blade tip extension angle (deg)
υ	kinematic viscosity (m^2/s)
ρ	air density (kg/m^3)
ω	angular velocity (rad/s)

Subscripts

ep	end plate
P	power
sh	rotor shaft
T	torque
w	wire

environments. The turbine also easily starts to rotate at low wind speeds because the differential drag on the two blades produces the torque. This allows the turbine to rotate not only at the top of high-rise buildings but also at street level in a city. As there are no severe restrictions on blade material, the manufacturing process is easy to realize on-site using on-site materials [3].

On the downside, Savonius turbines are widely considered as drag-driven devices [4]. The power extraction efficiency (power coefficient, C_p) from the wind is typically less than half of the efficiency of HAWTs and there are a number of geometrical parameters that affect this efficiency. Among the geometrical parameters of conventional Savonius rotors, the optimum overlap ratio value has been found as 0.15 by Fujisawa [5] in an experimental study, and Akwa et al. [6] in a numerical investigation. Open jet wind tunnel experiments at this value of overlap ratio and an aspect ratio of 1.0 have been reported to have a maximum power coefficient of 17.3% by Fujisawa and Gotoh [7] and 17% by Kamoji et al. [8]. This value corresponds to only one-third of maximum ideal power coefficient of 59.3% (Betz's limit). However, it has been observed that, at low angles of attack, the lift force also contributes to the overall torque generation [6,9,10]. Thus, it can be concluded that the Savonius rotor is a combination of a drag-driven and a lift-driven machine. Therefore, it can go beyond the limit of power coefficient of purely drag-driven devices which is 8% [11].

Continual efforts are being made to improve the coefficient of power either by examining the effects of various design parameters, by incorporating additional features, or by modifying the shape of conventional Savonius rotors. The number of rotor blades has significant effect on Savonius rotor performance [12]. Wind tunnel experiments show that the three blade rotor is inferior to the two blade rotor, while the performance of two stage rotor is superior to the single stage rotor [13,14]. Kamoji et al. [15] in an experimental study concluded that, double-step and three-step rotors are slightly superior to the corresponding single-step rotor in self-starting, but lower for

both torque and power characteristics. Further investigation on the single stage and three stage rotors in an open jet wind tunnel by Hayashi et al. [16] concluded that the static and dynamic torque variations in one revolution of three stage rotor are positive and smoother in comparison with the single stage Savonius rotor but that the aerodynamic coefficients of three stage rotors were much smaller than single stage rotors.

An Investigation on modified Savonius rotors was reported by Modi and Fernando [10] to have a maximum power coefficient of around 32% based on closed jet wind tunnel testing. Menet [17] proposed a modification of Savonius rotor using three geometrical parameters which has maximum values of static torque much higher than conventional rotor. Kamoji et al. [18] examined the influence of the end plates and the central shaft on a single stage modified Savonius rotor and found that the power coefficient rose up to 21% with the best combination. Mahmoud et al. [19] confirmed higher coefficient of power when end plates were used. Experiments on twisted Savonius rotor showed better performance than conventional semicircular rotor, but sensitive to Reynolds number [1,13]. Saha and Rajkumar [20] confirmed that the twisted blades in the vertical direction provide a better performance (13.99%) than conventional cylindrical blades (11.04%) at low air speeds. Reupke and Probert [21] performed dynamic-torque tests for Savonius wind rotor with hinged blades to improve the performance of the rotor. Roy and Saha [22] conducted wind tunnel experiments on a newly built two-bladed turbine and compared its performance with semi-circular, semi-elliptic, Benesh and Bach type bladed turbines that demonstrate a gain of 34.8% in maximum power coefficient compared to the conventional bladed Savonius turbine.

Another area of improvement presented by Ushiyama et al. [23] is the introduction of wind collection equipment to the space around Savonius wind turbines. Surrounding the turbine with a guide box succeeded in raising the power coefficient by up to 123% for two-blade and 150% for three-blade models relative to the original models reported by Irabu and Roy [24]. Mohamed et al. [25] placed an obstacle plate in front of

the returning side of the rotor for better flow orientation towards the advancing blade. They observed that their optimized design increases the power coefficient by more than 27%, better starting capability, and higher torque coefficient. Furthermore, Ogawa et al. [26] investigated the use of a deflecting plate and found that the rotor power was approximately 30% greater than that of a rotor without the deflecting plate. In a similar manner, further significant success was reported by Altan et al. [27] using mobile types of solid curtains that recorded 38% for the maximum power coefficient. These large improvements are considered to be due to the drag reduction on the returning blade that migrates upstream against the main flow.

Recently, Al-Faruk et al. [28] proposed an innovative low cost technique of performance improvement of Savonius turbines using hot air sourced from either industrial waste heat or natural heat sources. They numerically investigated the possibility of combining the fire-whirl mechanism with the primary Savonius wind turbine mechanism by modifying the blade geometry in a new design (naming the new configuration as swirling Savonius). They reported that swirling flows were formed in the vortex chamber, and the comparison between the conventional and swirling Savonius revealed increase in angular speed and power coefficient of the swirling Savonius turbine. Later, Al-Faruk and Sharifian [29] confirmed performance improvement of the swirling Savonius turbine by a preliminary experimental investigation using industrial pedestal fan. However, due to the high uncertainty of the experiment, mainly caused by the non-uniformity ($\pm 8\%$) of the freestream wind from the fan, the results were considered to be unreliable and inconclusive.

In the present study, experimental investigations were carried out on the proposed configuration of the swirling Savonius rotor to obtain a geometrically optimal rotor using an open jet wind tunnel with minimal uncertainty. Several design parameters such as blade overlap ratio, blade arc angle, diameter of hot air inlet, rotor aspect ratio, and condition of the top end plate of the swirling chamber were considered to determine their effects on the aerodynamics performances in terms of coefficient of power and coefficient of torque. The existing arrangement of experimental set-up allowed the performance assessment of the swirling Savonius rotor as well as conventional Savonius rotor in different wind velocities.

2. Experimental set-up

The experimental set-up consisted of a structural test bench housing the swirling Savonius rotor and hot air generation chamber, wind tunnel, and measurement devices. The swirling Savonius turbine is similar to the classic Savonius turbine that consists of two identical blades of semi-cylinder like surfaces which are moved sideways and overlap, as shown in Fig. 1. The modification made in the swirling Savonius turbine is that, the inner tips of the half cylindrical blades extended further to construct a swirling chamber [28,29]. This makes larger blade arc angle of the swirling Savonius rotor than the conventional Savonius rotor. The extended angle (θ) of the blades, as shown in Fig. 1, lowers the air entrainment gap of the vortex chamber. A circular hole of diameter d made in the bottom end plate acts as the hot air inlet of the swirling chamber. The blade overlap ratio (β) of the swirling Savonius turbine can be defined as the ratio of blade overlap distance (e) and the inside diameter (ID) of the blade. The diameter of the rotor can be calculated using the inside and outside diameters of the blade pipe and the blade overlap ratio from $D = OD + ID(1 - \beta)$ formula. As the end plate diameter is usually made 10% larger than the rotor diameter for the conventional Savonius turbine with optimum performance [30], the same ratio was applied to the new rotor.

The wind tunnel used in the experiments was an open-jet type driven by two contra rotating fans. Air exited from a circular outlet of 50 cm diameter. The wind velocity could be changed by blocking the passage in the suction side, or with the use of an adjustable damper in the wind tunnel. The test bench was placed at 3.06 m distance downstream of the wind tunnel exit such that the centre of the rotor was in line with the centre of the wind tunnel in order to obtain uniform flow (see Fig. 2). The rotor and several measuring devices were placed on top of the bench and the heating chamber was placed underneath the table (see Fig. 3).

Light weight and transparent Acrylic tube of 180 mm outside diameter and wall thickness of 3 mm was chosen as the blade material. The bottom end plate was made from 3 mm thick Aluminium sheet, and 3 mm Acrylic sheet was used as the top end plate to provide a clear view of the rotor. Circular holes of 24 mm and 100 mm diameter were cut at the centre of the bottom and top end plates, respectively, as shown in Fig. 1. The bottom hole acted as the hot air inlet of the chamber and the top hole provided an opening to the vortex chamber. Blade shape grooves were etched on the end plates to ensure a robust assembly. As a result, four pairs of end plates for four different blade overlap ratios were used. After inserting the ends of the blades into the grooves of the end plates, strong adhesive was used to complete the fabrication of the rotor. The blade overlap ratios, blade overlap distances, and rotor diameters used in this study are listed in Table 1.

The bottom end plate of the turbine was coupled with the end flange of an Aluminium hollow shaft and placed into a fixed ball bearing on the test bench. A 50 mm diameter stainless steel pipe was used as a chimney that carried the warm air from the hot air chamber and into the swirling chamber. The heating zone at the bottom of the test table was fabricated using 0.9 mm Stainless Steel sheet. Two cooking hot plates were used for heating the air. Only hot surfaces of the heating plates sat inside the enclosure due to safety concerns. To minimize heat loss to the environment from the hot air enclosure and the chimney, room insulation batts were used to cover outer surfaces. A 250 mm × 200 mm opening with sliding cover was made in the side wall to allow and control the entry of fresh air into the chamber.

A K-type thermocouple was inserted through a hole at the top end of the chimney to measure temperature of the warm air entering into the swirling chamber of the rotor. A hot wire anemometer was used to measure wind velocity and a brake rope dynamometer was used to apply brake load on the Savonius rotor and to measure the rotor torque. The brake rope dynamometer consisted of a weighing pan, two pulleys and a spring balance. The weighing pan and the spring balance were connected by a fishing nylon string of 0.4 mm diameter running over the pulleys. The string was wounded one turn (360°) over the hollow shaft of the rotor on the top of the bearing housing.
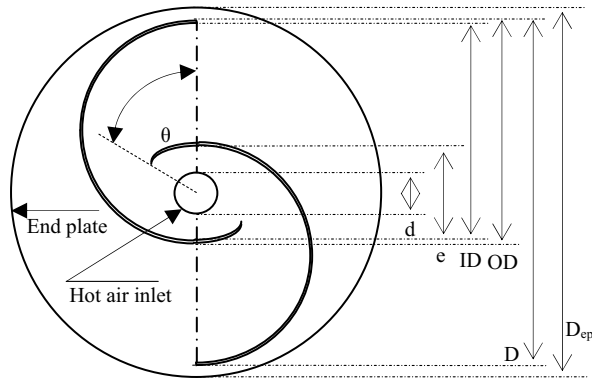
(a) Blade geometry onthe bottom end plate　　　　　　　　　　　(b) Photographic view
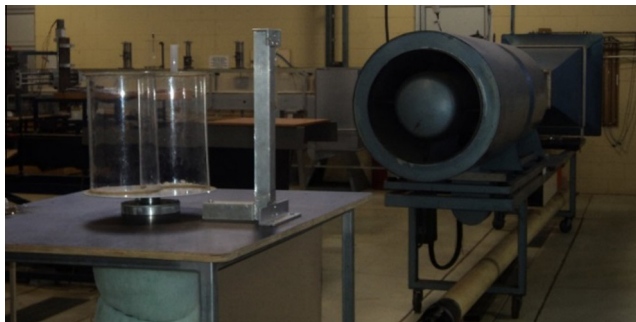
Figure 1　The swirling Savonius rotor.

Figure 2　Photograph of the experimental test bench and the wind tunnel.

3. Experimental measurements and data acquisition

The test bench was placed at 3.06 m downstream from the wind tunnel exit such that the centre of the rotor was in line with the centre of the tunnel exit to allow sufficient distance for the wind to become uniform at the rotor plane and to minimize the experimental error. Steady free stream flow is also necessary for the stability of the swirling flows inside the vortex chamber as well as to reduce the fluctuations of rotor angular velocity. To minimize error during the wind velocity measurements, the hot wire anemometer was fixed to the test bench using a stand and G-clamp, as shown in Fig. 4. Wind velocities at 50 cm upstream and 50 cm downstream from the central axis of the rotor were measured at 9 points located systematically in
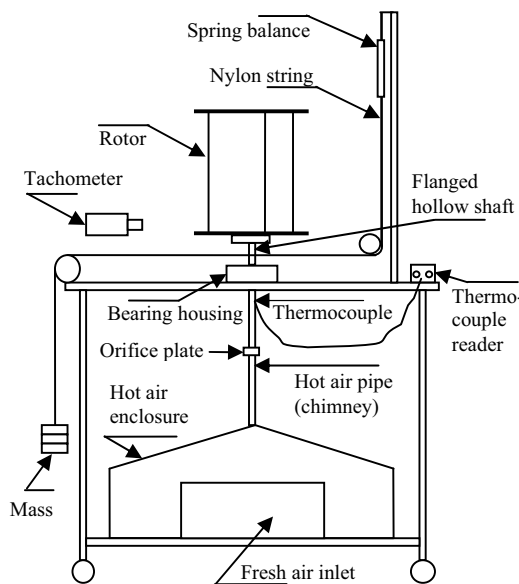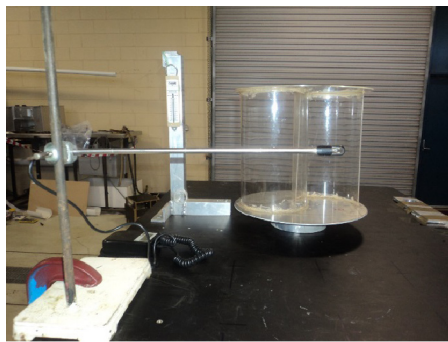

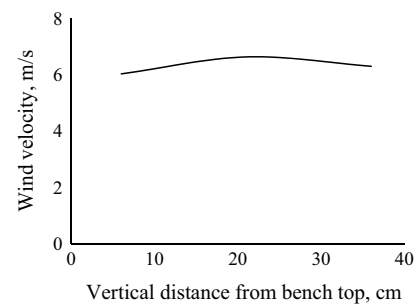(a) Schematic view　　　　　　　　　　　　　　　　　　　(b) Photographic view

Figure 3　Experimental set-up.

Table 1 Rotors covered in this study with dimensions corresponding to blade overlap ratios.

Turbine Type	Blade overlap ratio (β)	Blade overlap distance (e) mm	Rotor diameter (D) mm	Rotor height (H) mm	Rotor aspect ratio (H/D)	Blade arc angle
Conventional Savonius	0.15	26.0	328.0	328	1.0	180°
Swirling Savonius	0.20	34.8	319.2	168	0.52	190°
				242	0.78	195°
				300	0.94	200°
				337	1.06	
	0.25	43.5	310.5	168	0.52	190°
				242	0.78	195°
				300	0.94	200°
				337	1.06	
	0.31	54.0	300.0	168	0.52	190°
				242	0.78	195°
				300	0.94	200°
				337	1.06	

(a) (b)

Figure 4 (a) Wind velocity measurement set-up by hot wire anemometer, and (b) velocity distribution at 50 cm upstream along rotor axis.

the projected area of the rotor. The projected area of the rotor were divided into 3×3 equal distant grid points where the wind velocities were measured. Then the average value of each projected area was averaged to obtain the wind velocity which was used to calculate the performance parameters. The measured velocity distribution at 50 cm upstream of the rotor along the central axis was uniform within $\pm 5\%$, as presented in Fig. 4(b).

The rotors were allowed to rotate from no load condition, and the rotational speed (ω) was recorded by a digital tachometer when the rotor reached a steady state (periodic) condition. The rotors were loaded gradually (adding 50 g of mass each time) by the rope brake dynamometer from the no load condition to the highest load that stopped the rotor. The spring balance readings (S) and the dead weights (W) of the dynamometer were recorded and used to calculate the brake torque (T) and brake power (P) of the rotor at each loading condition using the following formula:

$$T = \frac{(D_{sh} + d_w)}{2} \times (W - S) \qquad (1)$$

$$P = T \cdot \omega \qquad (2)$$

where D_{sh} is the diameter of the rotor shaft and d_w is the nylon wire diameter.

The dimensionless performance parameters used in the aerodynamics of wind turbines are coefficient of power and coefficient of torque, which are usually determined as a function of dimensionless tip speed ratio (γ).

$$C_p = \frac{P}{\frac{1}{2}\rho DHU^3} \qquad (3)$$

$$C_t = \frac{T}{\frac{1}{4}\rho D^2 HU^2} \qquad (4)$$

$$\gamma = \frac{\omega D}{2U} \qquad (5)$$

where ρ is the air density, U wind velocity, H rotor height, and D rotor diameter.

3.1. Uncertainty analysis of experiments

The relative uncertainties of the independent or measurable parameters in the experimental study were determined first and it was found that the uncertainties were very low except

for rotor angular speed (2.7%) and wind velocity (7.1%). Then the relative uncertainties of the dependent parameters were estimated based on the functional form of the independent parameters from the general uncertainty formula presented by Bevington and Robinson [31]. The relative uncertainty of the torque and power coefficients were found to be 21.5% and 21.7%, respectively.

4. Results and discussions

A series of experimental tests were carried out over 30 swirling and conventional Savonius rotors with various geometrical parameters and wind velocities in an open jet wind tunnel. The design parameters studied in these experiments were the blade overlap ratio, blade arc angle, rotor aspect ratio, diameter of hot air inlet, and the condition of the top opening of the swirling chamber. The results were analysed based on the influence of these parameters on the performance of the swirling Savonius rotor to obtain an optimum geometry in terms of maximum coefficient of power. After obtaining the optimum geometry, the effects of the free-stream wind velocity on the power coefficient were tested at four different Reynolds numbers based on the rotor diameter. Finally, the performance of the optimum conventional Savonius rotor was determined under the same experimental conditions in order to compare the results with those of the optimum swirling Savonius rotor.

4.1. Condition of top end plate

The influence of a 100 mm diameter opening at the top end plate was investigated for four pairs of swirling Savonius rotors with and without the opening at different aspect ratios ranging from 0.52 to 1.06. The coefficients of power and torque were plotted versus the blade tip speed ratio in Fig. 5 at 0.20 blade overlap ratio (34.8 mm overlap between the blades), 200° blade arc angle, 0.94 rotor aspect ratio, 22 mm hot air inlet, and 4.9 m/s free stream wind velocity.

The results show that the performance improves when the top opening is closed and the maximum power coefficient found in this case was 21.15% at 0.62 tip speed ratio. The maximum coefficient of power occurred at 34.10% torque coefficient. On the other hand, the maximum coefficient of power
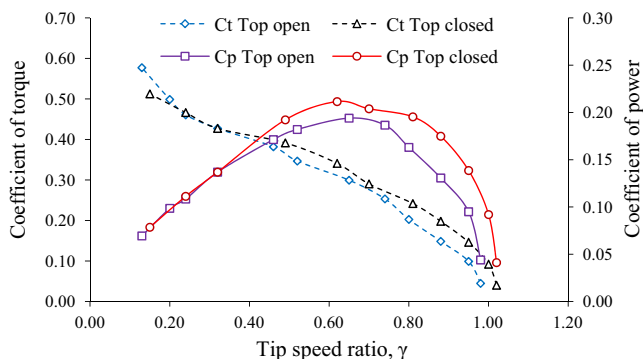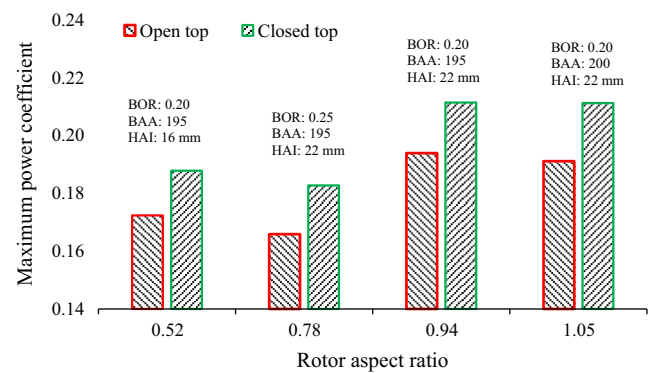

Figure 5 Comparison of power and torque coefficients with and without top opening of swirling Savonius rotor at 0.20 blade overlap ratio, 200° blade arc angle, 22 mm diameter of hot air inlet and 0.94 rotor aspect ratio.

BOR is blade overlap ratio, BAA is blade arc angle, HAI is hot air inlet diameter

Figure 6 Comparison of maximum power coefficients with and without top end plate opening at four rotor aspect ratio and 4.90 m/s wind velocity.

obtained for the top open case was 19.40% at 0.65 tip speed ratio and 29.95% coefficient of torque. The reason of lower performance is perhaps the loss of pressure through the top opening. The results are the same for all the four cases but not conclusive because the relative uncertainty (21.7%) in power coefficient is higher than the difference of the maximum power coefficients between the two cases (9%).

The bar chart presents the maximum coefficient of power with and without the top opening at four different rotor aspect ratios (Fig. 6). The maximum power coefficients are larger with closed top end plates than their counterparts in all four cases of aspect ratio. However, the difference between the maximum values decreases at lower aspect ratio as shown in Fig. 6. The swirling flow does not reach the top of the rotor with a high aspect ratio, and this might be the reason for larger difference between the two power coefficients.

4.2. Effects of design parameters

The blade overlap ratios (β), defined by the ratio of blade overlap distance and the inner diameter of the blade (refer to Fig. 1), studied in these experiments were 0.15, 0.20, 0.25, and 0.31. The rotor dimensions corresponding to the blade overlap ratio are presented in Table 1.

The maximum power coefficients of the swirling Savonius turbines with respect to the blade overlap ratio for the four diameters of hot air inlet are plotted in Fig. 7. The maximum power coefficient of the swirling Savonius rotor found in this study is 21.56% occurring at 0.20 blade overlap ratio, 16 mm hot air inlet diameter, and 195° blade arc angle. The results indicate that the optimum value of blade overlap ratio is 0.20 for the swirling Savonius turbine as the maximum power coefficient was obtained at this value for all the cases of swirling Savonius turbine contrary to 0.15 for the conventional Savonius turbine. In all the cases of hot air inlet diameter, the maximum power coefficient decreases with the increase of blade overlap ratio above the optimum value for the swirling Savonius turbine.

The variation of maximum power coefficient with the diameter of hot air inlet for the four blade overlap ratios is plotted in Fig. 8. From the plot, it is evident that the maximum power coefficients at 0.20 blade overlap ratios are higher compared to
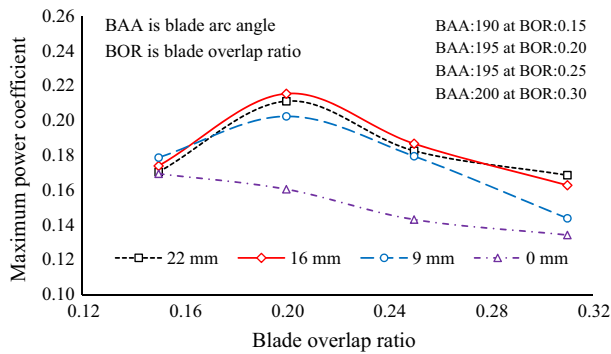
Figure 7 Variation of maximum power coefficients with different blade overlap ratios at 1.06 rotor aspect ratio, closed top end plate and 4.9 m/s wind velocity.
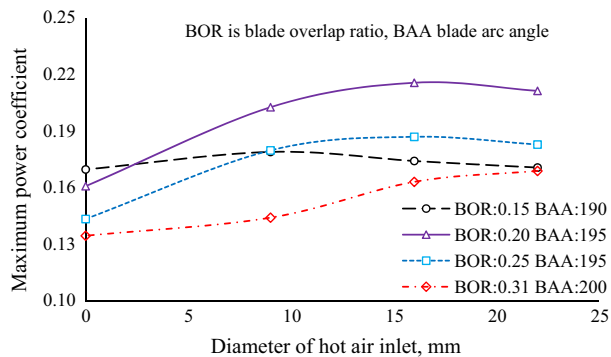

Figure 8 Maximum coefficients of power with diameter of hot air inlet at four different blade overlap ratios with closed top end plate, 1.06 rotor aspect ratio, and 4.9 m/s wind velocity.

the others for all diameters of the hot air inlet. The difference of maximum power coefficients between the blade overlap ratios of 0.20 and 0.31 at 16 mm hot air inlet is higher (32.3%) than the uncertainty of power coefficient (21.7%).

The diameter of the rotor depends on blade overlap ratio for the same inside and outside diameters of the rotor blade by the $D = OD + ID(1 - \beta)$ formula. So, with the increase of blade overlap ratio, the positive moment generating the concave blade's swept area reduces but the negative convex blade's swept area remains constant which results in lower overall moment on the shaft of rotor. For this reason, C_P reduces with the increase of blade overlap ratio after reaching the optimal value which is 0.15 for the conventional Savonius turbine. As swirling flow is generated in the blade overlapping zone of the swirling Savonius turbine, this compensates the loss of net moment due to the higher overlap ratio as well as promoting the performance up to 0.20 blade overlap ratio.

The diameter of the circular hole at the bottom end plate which is the hot air inlet of the swirling chamber was initially 22 mm. The other diameters tested in the experiments were 16, 9, and 0 mm. The maximum power coefficients versus the ratio of hot air inlet diameter and blade overlap distance (d/e) for two blade arc angles of 195° and 200°, and two blade overlap ratios of 0.20 and 0.25 have been plotted in Fig. 9. The results indicate that the maximum power coefficients are optimum for a certain value of hot air diameter to blade overlap ratio. In
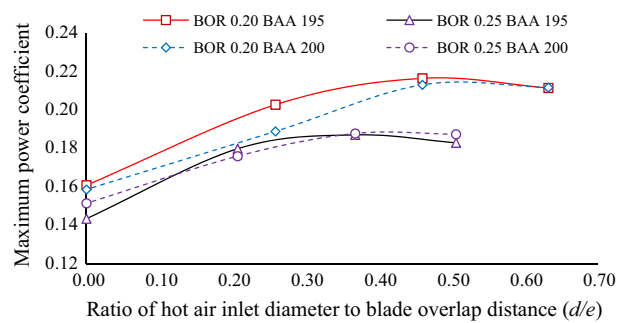

Figure 9 Variation of maximum power coefficient with hot air inlet diameter to blade overlap distance ratio for different blade arc angles (BAAs) and blade overlap ratios (BORs) with closed top end plate and 1.06 rotor aspect ratio.

this experiment, power coefficient reached maximum for 16 mm diameter of hot air inlet for all the cases which is about 0.45 of hot air inlet diameter to blade overlap distance ratio (d/e). The change of maximum power coefficients between the highest and lowest values at of 0.45 and 0 ratios of hot air inlet diameter to blade overlap, respectively is about 36% at 0.20 blade overlap ratio and 195° blade arc angle. The change in maximum C_p values is significant compared to the estimated uncertainty in power coefficient of the experiment.

Fig. 10 presents the maximum power coefficients of the swirling Savonius rotor for two blade overlap ratios of 0.20 (solid line) and 0.25 (broken line) with 16 mm diameter of hot air inlet for three different blade arc angles ranging from 190° to 200° as well as conventional 180° rotor. With the increase of blade arc angle, the power coefficient increases but after reaching a maximum value, it declines. Increasing the blade arc angle reduces the width of the air entrance passage, which results in a higher velocity of entrant air that generates a strong swirling flow. Perhaps it is the reason of high power coefficients. However, after the maximum point, the increase of blade arc angle increases the mass and the mass moment of inertia of the rotor and at the same time may create a blockage to the air flow between the blades; which may be the reason for the lower power coefficient. Therefore, the optimum blade arc angle is a trade-off between the increase of entrant air velocity in the swirling chamber and the blockage
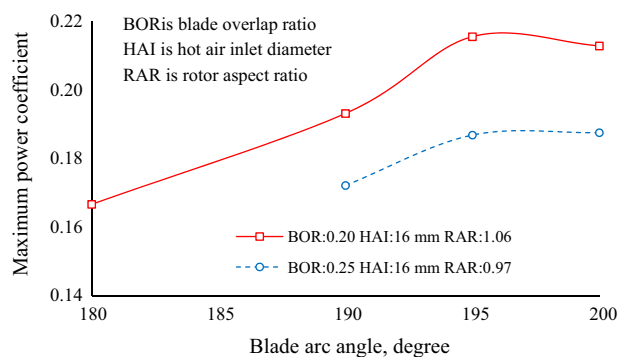

Figure 10 Effects of blade arc angle on maximum power coefficient at 16 mm hot air inlet diameter with closed top end plate and 4.9 m/s wind velocity.

effect due to the reduction of passage width caused by the blade tip extension.

The change of maximum power coefficient by reducing the blade arc angle from 195° to 180° is about 29% at 0.20 blade overlap ratio and 16 mm hot air inlet diameter.

To determine the influence of the rotor aspect ratio, which is defined as the ratio of the rotor height to the rotor diameter, four different rotors of 168, 242, 300, and 337 mm height and 319 mm diameter were used in this study. The above rotors were tested at 4.9 m/s wind velocity, keeping other geometrical parameters such as blade overlap ratio, blade arc angle, hot air inlet diameter, and closed top end plate constant. The plot of maximum coefficient of power versus rotor aspect ratio (Fig. 11) demonstrates that maximum power coefficient increases with the increase of rotor aspect ratio. Perhaps the reason for this is the lower specific mass (mass per unit frontal area) of high aspect ratio rotors than that of the high aspect ratio rotors with the same geometry, which results in a higher coefficient of power. The maximum C_p is around 14% higher at a rotor aspect ratio of 1.06 than 0.52.

4.3. Influence of wind velocity

After determining the influences of geometrical parameters on the coefficients of power, the optimum swirling Savonius rotor featuring 0.20 blade overlap ratio, 195° blade arc angle, 16 mm diameter of hot air inlet, and 1.06 aspect ratio rotor was tested in four different free stream wind velocities, to obtain the influence of the wind velocity on the power coefficient. The wind velocities were obtained by changing the damper position of the wind tunnel. The wind velocities used in this experiment were 4.12, 4.90, 5.58, and 6.24 m/s (which correspond to the Reynolds Number of 77,359, 92,005, 104,773, and 117,165), respectively. The Reynolds number is defined based on free-stream wind speed and rotor diameter. The maximum power coefficients against the wind velocities are plotted in Fig. 12. The best fitting cubic polynomial curve shown in Fig. 12 demonstrates that higher wind velocities yield larger power coefficients, and found that the power coefficient is around 6% higher at the maximum wind velocity of 6.24 m/s than at the minimum of 4.12 m/s tested in this experiment. This suggests that higher angular velocity of rotor or wind velocity is favourable for the generation of swirling flow.
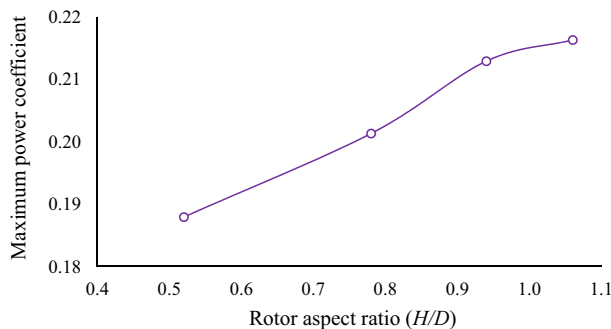
Figure 11 Effects of rotor aspect ratio on power coefficient at 0.20 blade overlap ratio, 195° blade arc angle, 16 mm hot air inlet diameter and 4.9 m/s wind velocity with closed top end plate.
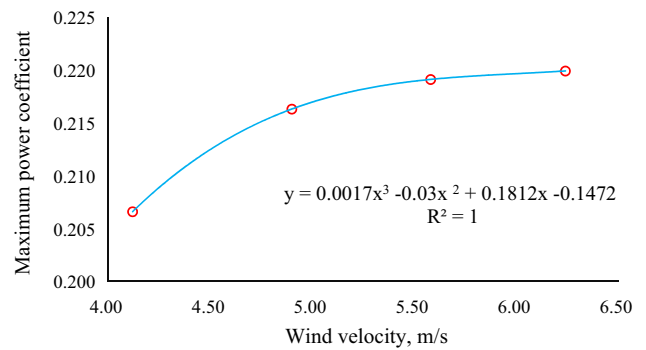
Figure 12 Effects of Reynolds number on maximum power coefficient at 0.20 blade overlap ratio, 195° blade arc angle, 16 mm hot air inlet diameter, and 1.06 aspect ratio with the closed top end plate.
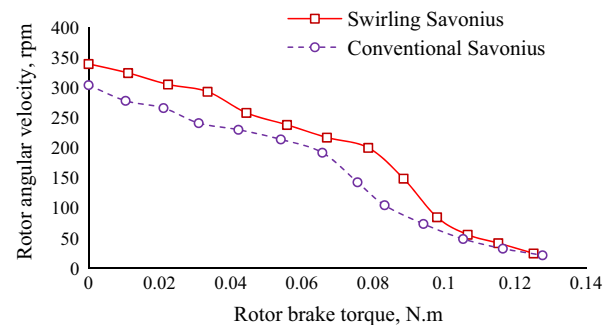
Figure 13 Variation of steady state angular velocity of conventional and swirling Savonius rotors with brake torque.

4.4. Comparison between conventional and swirling Savonius rotors

The best features of conventional and swirling Savonius turbines are compared in terms of steady state angular velocities, and power and torque coefficients.

The maximum steady state angular velocities versus brake torque of rotor are plotted in Fig. 13. The plot demonstrates that at no load, maximum angular speed of swirling rotor is higher (339 rpm) than the conventional rotor (304 rpm). With the increase of brake torque on the rotor, the differences in speed values drops and the values are almost the same before stopping. This performance suggests that swirling flow may not be generated at lower angular velocities but that it grows stronger with the increase of angular velocity.

Fig. 14 represents the coefficients of torque and power plotted against the tip speed ratios for optimum swirling and conventional Savonius turbines. The maximum torque coefficients for both turbines are nearly the same value of over 50%, but the differences extend at higher tip speed ratios. The highest tip speed ratio obtained at no load condition of swirling Savonius turbine is 1.1, which is 13% higher than that of conventional Savonius turbine. From those plots it can be deduced that, the swirling flow might not be generated at lower angular speeds of swirling Savonius turbine.

The plot of power coefficient versus rotor tip speed ratio for the optimum swirling and conventional Savonius rotors
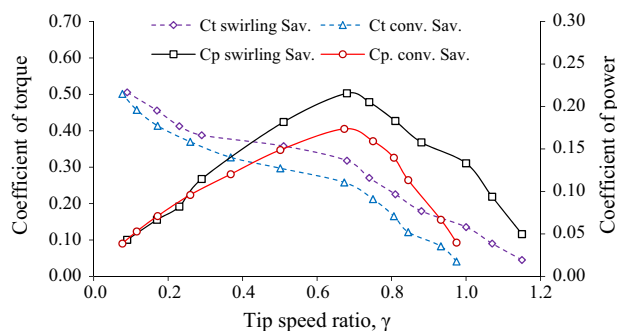
Figure 14 Variation of torque and power coefficients with tip speed ratio of a swirling rotor of 28 mm blade overlap, 16 mm diameter hot air inlet and 195° blade arc angle and the conventional Savonius rotor at 4.9 m/s wind velocity.

demonstrates that, at low tip speed ratios, the values are nearly the same, but the difference widens with the increase of steady state (periodic) speeds of the rotor. The maximum power coefficient (21.56%) was found at 0.68 tip speed ratio and 31.79% torque coefficients for swirling Savonius turbine whereas for Savonius turbine, the maximum power coefficient (17.37%) occurred at 0.67 tip speed ratio and 25.81% torque coefficient. The increase of power coefficients by 24.12% is a conclusive performance improvement of the swirling Savonius turbine compared to the conventional Savonius turbine as the measured relative uncertainty of 21.65% in this experiment for power coefficient is lower than improvement.

5. Conclusions

The optimum swirling Savonius wind turbine geometry has been obtained in terms of power coefficient by wind tunnel experiments, which is 0.20 blade overlap ratio, 16 mm hot air inlet diameter, 195° arc angle of the blades, and closed top of the swirling chamber. The optimum geometry of the swirling turbine, was then tested in different wind velocities to determine the effects of the Reynolds number on its performance. Performance investigation of conventional Savonius turbine was also conducted with the same experimental conditions to compare the performance of the two turbines. The following conclusions may be drawn from the present experimental study:

- The opening in the top of the swirling chamber has deteriorating effects on the performance of the swirling Savonius turbine perhaps due to the pressure loss through the opening. The deteriorating effects are less in the low aspect ratio rotor compared to the high aspect ratio rotor.
- The blade overlap ratio has the most significant effect on the performance. Power coefficient is maximum at 0.20 blade overlap ratio contrary to the 0.15 blade overlap ratio of the conventional Savonius rotor.
- The coefficient of power reaches a maximum at a certain value of hot air inlet diameter to blade overlap ratio.
- Power coefficients increase with the increase of blade arc angle up to a certain optimal value of 195° which is 29% higher than the conventional blade arc angle of 180°.

- A higher aspect ratio is preferred compared to a lower aspect ratio if other geometrical parameters remain the same.
- The coefficient of power, coefficient of torque and no load tip speed ratio of the swirling Savonius turbine marginally increase with the increase of wind velocity suggesting higher wind velocity is favourable for the generation of swirling flows.
- The comparison of performance between the optimum swirling and conventional Savonius turbines indicates that the power coefficient of the swirling turbine is conclusively improved because of the generation of swirling flow generated inside the turbine chamber. However, at lower angular velocities the performances of swirling and Savonius turbines are almost identical.

References

[1] A. Damak, Z. Driss, M.S. Abid, Experimental investigation of helical Savonius rotor with a twist of 180°, Renew. Energy 52 (2013) 136–142.
[2] R.E. Sheldahl, B.F. Blackwell, L.V. Feltz, Wind tunnel performance data for two- and three-bucket Savonius rotors, J. Energy 2 (1978) 160–164.
[3] L.-C. Valdès, J. Darque, Design of wind-driven generator made up of dynamos assembling, Renew. Energy 28 (2003) 345–362.
[4] S.J. Savonius, The S-rotor and its applications, Mech. Eng. 53 (1931) 333–338.
[5] N. Fujisawa, On the torque mechanism of Savonius rotors, Wind Eng. Ind. Aerodyn. 40 (1992) 277–292.
[6] J.V. Akwa, G.A.d.S. Júnior, A.P. Petry, Discussion on the verification of the overlap ratio influence on performance coefficients of a Savonius wind rotor using computational fluid dynamics, Renew. Energy 38 (2012) 141–149.
[7] N. Fujisawa, F. Gotoh, Experimental study on the aerodynamic performance of a Savonius rotor, J. Sol.Energy Eng. 116 (1994) 148–152.
[8] M.A. Kamoji, S.V. Prabhu, S.B. Kedare, Experimental investigations on the performance of conventional Savonius rotor under static and dynamic conditions, in: 3rd International Conference on Fluid Mechanics and Fluid Power, 2006.
[9] J.V. Akwa, H.A. Vielmo, A.P. Petry, A review on the performance of Savonius wind turbines, Renew. Sustain. Energy Rev. 16 (2012) 3054–3064.
[10] V.J. Modi, M.S.U.K. Fernando, On the performance of the Savonius wind turbine, J. Sol.Energy Eng. 111 (1989) 71–81.
[11] J.F. Manwell, J.G. McGowan, A.L. Rogers, Wind Energy Explained: Theory, Design and Application, second ed., John Wiley & Sons Ltd., Great Britain, 2009.
[12] I. Al-Bahadly, Building a wind turbine for rural home, Energy Sustain. Dev. 13 (2009) 159–165.
[13] U.K. Saha, S. Thotla, D. Maity, Optimum design configuration of Savonius rotor through wind tunnel experiments, J. Wind Eng. Ind. Aerodyn. 96 (2008) 1359–1375.
[14] I. Ushiyama, H. Nagai, Optimum design configurations and performance of Savonius rotors, Wind Eng. 1 (1988) 59–75.

[15] M.A. Kamoji, S.B. Kedare, S.V. Prabhu, Experimental investigations on single stage, two stage and three stage conventional Savonius rotor, Int. J. Energy Res. 32 (2008) 877–895.

[16] T. Hayashi, Y. Li, Y. Hara, Wind tunnel tests on a different phase three-stage Savonius rotor, JSME Int. J. Ser. B 48 (2005) 9–16.

[17] J.-L. Menet, Aerodynamic behaviour of a new type of slow-running VAWT, in: J. Peinke, P. Schaumann, S. Barth (Eds.), Wind Energy Proceedings of the Euromech Colloquium, Springer, Berlin Heidelberg, 2007, pp. 235–239.

[18] M.A. Kamoji, S.B. Kedare, S.V. Prabhu, Performance tests on helical Savonius rotors, Renew. Energy 34 (2009) 521–529.

[19] N.H. Mahmoud, A.A. El-Haroun, E. Wahba, M.H. Nasef, An experimental study on improvement of Savonius rotor performance, Alex. Eng. J. 51 (2012) 19–25.

[20] U.K. Saha, M.J. Rajkumar, On the performance analysis of Savonius rotor with twisted blades, Renew. Energy 31 (2006) 1776–1788.

[21] P. Reupke, S.D. Probert, Slatted-blade Savonius wind-rotors, Appl. Energy 40 (1991) 65–75.

[22] S. Roy, U.K. Saha, Wind tunnel experiments of a newly developed two-bladed Savonius-style wind turbine, Appl. Energy 137 (2015) 117–125.

[23] I. Ushiyama, H. Nagai, J. Shionoda, Experimentally determining the optimum design configuration for Savonius rotors, Trans. Jpn. Soc. Mech. Eng. Ser. B 52 (1986) 2973–2981.

[24] K. Irabu, J.N. Roy, Characteristics of wind power on Savonius rotor using a guide-box tunnel, Exp. Therm. Fluid Sci. 32 (2007) 580–586.

[25] M.H. Mohamed, G. Janiga, E. Pap, D. Thévenin, Optimization of Savonius turbines using an obstacle shielding the returning blade, Renew. Energy 35 (2010) 2618–2626.

[26] T. Ogawa, H. Yoshida, Y. Yokota, Development of rotational speed control systems for a Savonius-type wind turbine, J. Fluids Eng. 111 (1989) 53–58.

[27] B.D. Altan, M. Atilgan, A. Özdamar, An experimental study on improvement of a Savonius rotor performance with curtaining, Exp. Therm. Fluid Sci. 32 (2008) 1673–1678.

[28] A. Al-Faruk, A.S. Sharifian, S.R. Al-Atresh, Numerical investigation of performance of a new type of Savonius turbine, in: 18th Australasian Fluid Mechanics Conference, Launceston, Australia, 2012.

[29] A. Al-Faruk, A. Sharifian, Influence of blade overlap and blade angle on the aerodynamic coefficients in vertical axis swirling type Savonius wind turbine, in: 19th Australasian Fluid Mechanics Conference, Melbourne, Australia, 2014.

[30] J.-L. Menet, A double-step Savonius rotor for local production of electricity: a design study, Renew. Energy 29 (2004) 1843–1862.

[31] P.R. Bevington, D.K. Robinson, Data Reduction and Error Analysis for the Physical Sciences, McGraw-Hill, Crawfordsville, IN, 2003.